Phonon dynamics of NaI investigated by $G(r, E)$ analysis

Mitsutaka Nakamura[a,*], Tatsuya Kikuchi[a,b], Kazuya Kamazawa[c], Yukinobu Kawakita[a]

[a] *Materials and Life Science Division, J-PARC Center, Japan Atomic Energy Agency, Tokai, Ibaraki 319-1195, Japan*
[b] *Sumitomo Rubber Industries, LTD., Kobe, Hyogo 651-0072, Japan*
[c] *Neutron Science and Technology Center, Comprehensive Research Organization for Science and Society, Tokai, Ibaraki 319-1106, Japan*

Abstract

The phonon dynamics of NaI is investigated from the dynamical structure function in real-space $G(r, E)$ transformed from the $S(Q, E)$ measured by inelastic neutron scattering measurement. In this study we used the incident energies of 36.9 and 81.3 meV which cannot yield very large maximum momentum transfer Q_{max}. Our analyses have shown that the inelastic neutron scattering measurement under the conventional condition $Q_{max} \sim 5$ Å^{-1} can provide us a meaningful information on the phonon dynamics at around the first nearest neighbor distance of Na-I through the $G(r, E)$ analysis on accepting the worse real-space resolution.

Keywords: Phonon dynamics, Real space analysis, Alkali halide

1. Introduction

The dynamical structure function in real-space $G(r, E)$ is deduced from the dynamical structure factor $S(Q, E)$ which can be obtained from inelastic neutron scattering (INS) measurement. So far there have been several reports on the $G(r, E)$ analysis both from the theoretical and the experimental aspects through the INS measurement of amorphous boron [1], vitreous silica [2, 3], nickel [4, 5] , relaxor ferroelectric [5], $FeSe_xTe_{1-x}$ [6], $YTiO_3$ [7] and so on. In these experiments the $S(Q, E)$ up to very large momentum transfers ($Q \geq 20$ Å^{-1}) was needed to directly apply the Fourier transformation. It means that both the large amounts of sample and the long measurement time are indispensable. Consequently, the dynamical study utilizing $G(r, E)$ analysis has not yet become widespread.

To extract more physical information from INS measurement under the conventional experimental conditions, however, it should be important to examine how the $G(r, E)$ deduced from such $S(Q, E)$ can contribute to the dynamical study of materials although the physical limitation of the worse real-space resolution coming from the limited maximum momentum transfer Q_{max} must be accepted. In this study, we have chosen the polycrystalline NaI as a standard sample. NaI is one of the most famous alkali halide crystals, and has the NaCl structure at a lattice constant of 6.46 Å [8]. The large difference in mass between the constituent atoms gives rise to the large phononic band gap between the acoustic and optic phonon branches [9]. These characteristic properties surely help us to evaluate the $G(r, E)$ features associated with the respective phonon modes. So far there have been various studies over the presence of intrinsic localized modes in NaI crystal [10, 11, 12, 13, 14, 15]. But this has no connection with the main subject of this paper.

2. Analysis method

The dynamical structure factor $S(Q, E)$ can be separated into distinct and self-scattering functions as follows:

$$S(Q, E) = S_d(Q, E) + S_s(Q, E), \quad (1)$$

where the distinct term $S_d(Q, E)$ is defined by

$$S_d(Q, E) = 4\pi \int G(r, E) \frac{\sin Qr}{Q} dr + B(Q, E), \quad (2)$$

where the $G(r, E)$ has the dimension of atomic pair distribution function (PDF). The $B(Q, E)$ involves the spherical Bessel function of the second kind $j_2(x)$. Previously, as Hannon *et al.* demonstrated [1], the effect of $j_2(x)$ term on the Fourier transform is principally on the leading edge of the peak. We assume that the $B(Q, E)$ term in Eq. (2) can be negligible in calculation.

*Corresponding author. Tel: +81 29 284 3198
Email address: mitsutaka.nakamura@j-parc.jp (Mitsutaka Nakamura)

The self term $S_s(Q,E)$ can be assumed to be simply expressed by aQ^2. Thus the Eq. (1) is generalized to

$$S(Q,E) = 4\pi \int G(r,E)\frac{\sin Qr}{Q}dr + aQ^2 + c, \quad (3)$$

where c is the constant background.

In our calculations, we define the kth calculated dynamical structure factor $S_{cal}(Q_k,E)$, given as

$$S_{cal}(Q_k,E) = 4\pi \sum_i G(r_i,E)\frac{\sin Q_k r_i}{Q_k} + aQ_k^2 + c. \quad (4)$$

The free energy constraint is introduced as

$$F = \frac{1}{2}\sum_k \frac{\{S_{obs}(Q_k,E) - S_{cal}(Q_k,E)\}^2}{\sigma_k^2} - \alpha\left[\sum_i \{G(r_i,E)\}^2 + \gamma(a^2+c^2)\right]^2, \quad (5)$$

where $S_{obs}(Q_k,E)$ is the kth observed dynamical structure factor and σ_k the standard deviation of $S_{obs}(Q_k,E)$. The γ is assumed to be infinitesimal, thus this contributions are negligible in calculation. The second term of Eq. (5) is related to the so-called information entropy, where α is determined to maximize the conditional probability $P(\alpha|S_{obs}(Q_k,E))$. The most probable $G(r,E)$ will be solved by the iteration to minimizing F at a specific α. The calculations were performed with our in-house code which was written in Igor Pro language under Igor Pro ver. 6 (WaveMetrics Inc., USA).

3. Experimental procedures

The INS measurements were performed on the Fermi chopper spectrometer 4SEASONS [16] at the Materials and Life Science Experimental Facility in the Japan Proton Accelerator Research Complex (J-PARC). We selected the incident energies of 36.9 and 81.3 meV with the chopper frequency of 250 Hz, where the energy resolutions at elastic scattering were 1.9 and 5.6 meV, respectively. These incident energies were simultaneously selected using the so-called multi-E_i method [17]. The beam power of the J-PARC was 218 kW at the time we carried out this study. The data reduction processes were completed by using Utsusemi suite [18]. The prepared NaI sample was in the polycrystalline powder form which was purchased from Wako Pure Chemical Industries. Approximately 15.8 g of the sample was wrapped in an aluminum foil and kept in the aluminum can with He exchange gas. Sample temperature was controlled to be at around 290 K by a top-loading closed-cycle refrigerator.

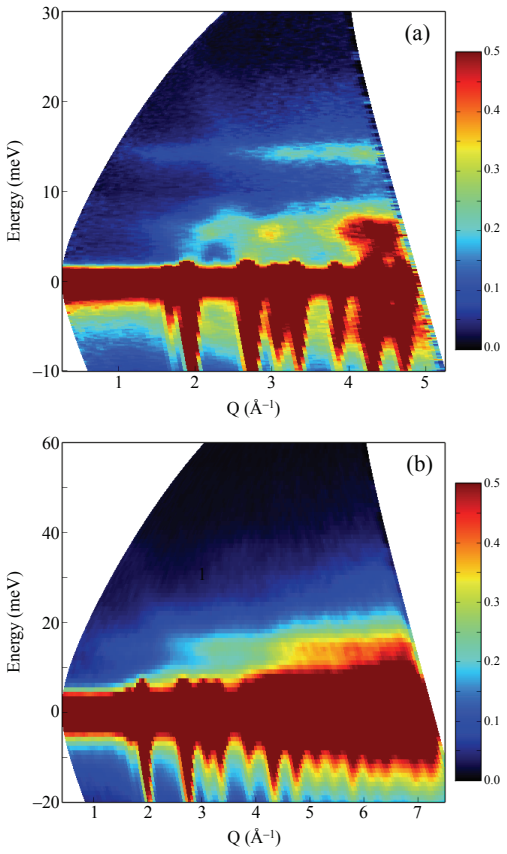

Figure 1: The dynamical structure factor $S(Q,E)$ of polycrystalline NaI measured by the incident energy of (a) 36.9 meV and (b) 81.3 meV.

4. Results and discussion

The two-dimensional $S(Q,E)$ maps of polycrystalline NaI are shown in Fig. 1(a) and 1(b). The incident energies for Fig. 1(a) and 1(b) are 36.9 meV and 81.3 meV, respectively. In Fig. 1(a) the transverse optic phonon mode is clearly observed at around 15 meV, while the acoustic phonon modes are densely observed below 10 meV. The $S(Q,E)$ measured by 81.3 meV incident energy covers a wide Q-E range although the inelastic features become obscured.

Figures 2(a) and 2(b) show the $G(r,E)$ maps at around the elastic region transformed from the $S(Q,E)$ maps in Fig. 1(a) and 1(b), respectively. The respective r-dependences of $G(r,E)$ are compared in Fig. 2(c), where the integration width was $E = 0 \pm 5$ meV for each spectrum. The first, second and third nearest neighbor distances of Na-I are 3.23, 5.59, 7.22 Å, and those distances of Na-Na (I-I) are 4.57, 6.46 and 7.91 Å.

As shown in Fig. 2(c), several peaks corresponding to the nearest neighbor distances in NaI structure are observed. We may say that the $G(r, E)$ with 81.3 meV incident energy can correctly provide the peaks at least up to the second nearest neighbor distances. It is certainly not surprising that the $G(r, E)$ with higher incident energy can provide more precise peak features in higher r region because the INS measurement with higher incident energy yields higher Q_{max}. However, the point we would like to stress in this study is that even the $G(r, E)$ obtained by the $S(Q, E)$ under the conventional experimental condition ($Q \lessapprox 7$ Å^{-1}) has a potential to yield a meaningful information on the interatomic distances of a certain material.

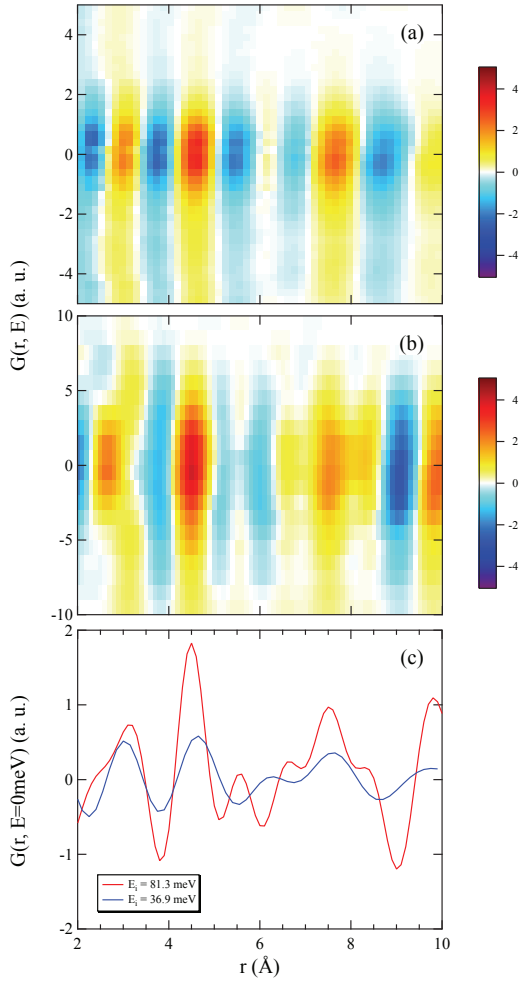

Figure 2: The $G(r, E)$ maps at around the elastic region transformed from the $S(Q, E)$ maps with the incident energies of (a) 36.9 meV and (b) 81.3 meV. (c) The r-dependences of $G(r, E)$ in elastic region.

Next, we shall discuss the characteristic features of $G(r, E)$ in the inelastic region. Figure 3(a) shows the energy dependences of $S(Q, E)$ measured by the incident energies of 36.9 and 81.3 meV, where the integrated Q range for both was from 2 to 4 Å^{-1}. The respective energy values of transverse acoustic (TA), longitudinal acoustic (LA) and transverse optic (TO) phonon modes are indicated by the arrows in the figure. In case of 81.3 meV incident energy, the acoustic phonon features are hidden by the tail of elastic scattering, and only TO phonon mode can be observed. In Fig. 3(b) the r-dependences of $G(r, E)$ at the energy region of TO phonon mode are compared. The phase of oscillation for both are considered to be quite similar although the measurement with higher incident energy gives sharper r profiles. Accordingly, it seems reasonable to discuss the dynamical properties of NaI only at around the first nearest neighbor distance of Na-I using the $G(r, E)$ with 36.9 meV incident energy.

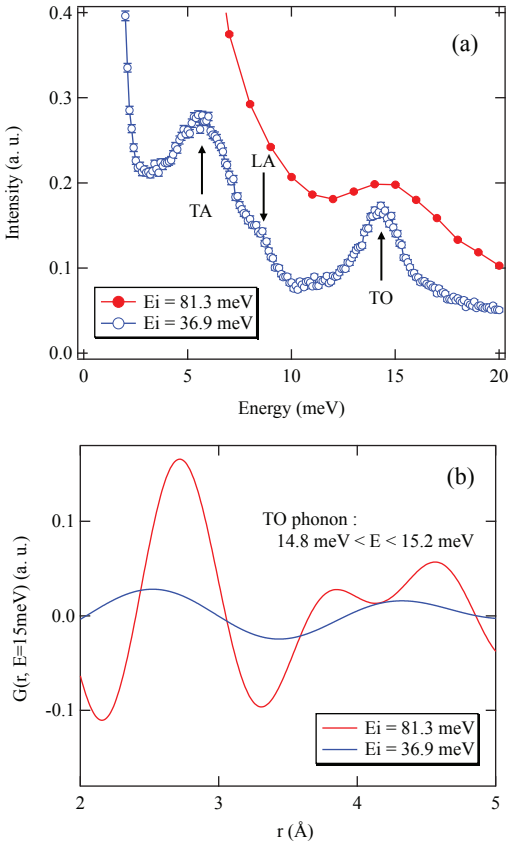

Figure 3: (a) The energy dependences of $S(Q, E)$ measured by the incident energies of 36.9 and 81.3 meV. (b) The r-dependences of $G(r, E)$ at the energy region of TO phonon mode transformed from the $S(Q, E)$ maps with the incident energies of 36.9 and 81.3 meV.

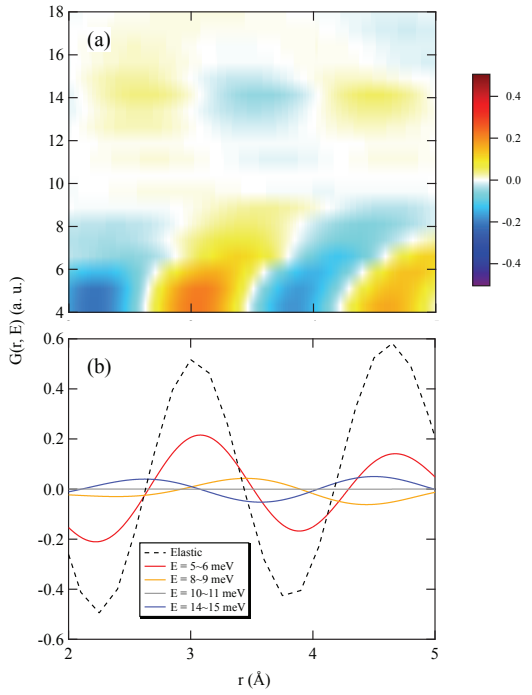

Figure 4: (a) The inelastic features of $G(r, E)$ transformed from the $S(Q, E)$ with 36.9 meV incident energy. (b) The r-dependence of $G(r, E)$ in several energy regions.

The inelastic $G(r, E)$ with 36.9 meV incident energy is given in Fig. 4(a), which may be divided into three regions, that is, acoustic ($4 < E < 9$ meV), phononic band gap ($9 < E < 12$ meV), and optic region ($12 < E < 18$ meV). The representative 1d-plots for each region are shown in Fig. 4(b). The 1d-plot for elastic region is also given in the figure. In acoustic region, the peak corresponding to the first nearest neighbor distance of Na-I (3.23 Å) tends to shift toward higher r with increasing energy. Looking further in detail, it is likely that there is almost no change in the peak position at $r \sim 3$ Å until $E = 6$ meV which must be interpreted that the first nearest neighbor Na and I tends to move in the same direction. Furthermore it is noteworthy that the $G(r, E)$ profiles of both the top of acoustic ($E = 8 \sim 9$ meV) and the optic region become zero at the r corresponding to the first nearest neighbor distance of Na-I. The $G(r, E)$ at $E = 8 \sim 9$ meV may correspond to the LA phonon mode at zone boundary (ZB). We suppose that these results indicate the constituent atoms (Na for acoustic and I for optic) are at rest in the respective energy ranges. The anti-phase behaviors of the $G(r, E)$ between LA at ZB and TO is also physically reasonable in terms of the phonon dynamics in polycrystalline NaI.

5. Conclusion

The dynamic structure factors in real space $G(r, E)$ of polycrystalline NaI were investigated. A series of $G(r, E)$ were transformed from the $S(Q, E)$ measured by INS experiments under the conventional conditions with the incident energies of 36.9 and 81.3 meV. The $G(r, E)$ analysis successfully provided us the physically reasonable results on the phonon dynamics of NaI at around the first nearest neighbor distance of Na-I. These results suggest the possibility that a large number of $S(Q, E)$ data which have been accumulated so far can be effectively reused. We will continue to investigate the phonon dynamics and the associated atomic motions in various kinds of materials using the $G(r, E)$ analysis.

Acknowledgments

The authors would like to express their gratitude to the technical support team of J-PARC Center and the instrument group staff of BL01 for help with the measurements. The experiments on 4SEASONS were performed under the user program 2013P0901.

[1] A.C. Hannon, M. Arai, R.G. Delaplane, Nucl. Instrum. Methods Phys. Res. Sect. A 354 (1995) 96.
[2] A.C. Hannon, M. Arai, R.N. Sinclair, A.C. Wright, J. Non-Cryst. Solids 150 (1992) 239.
[3] M. Arai, A.C. Hannon, T. Otomo, A. Hiramatsu, T. Nishijima, J. Non-Cryst. Solids 192&193 (1995) 230.
[4] R.J. McQueeney, Phys. Rev. B 57 (1998) 10560.
[5] W. Dmowski, S.B. Vakhrushev, I.-K. Jeong, M.P. Hehlen, F. Trouw, T. Egami, Phys. Rev. Lett. 100 (2008) 137602.
[6] K. Park, J.W. Taylor, D. Louca, J. Supercond. Nov. Magn. 27 (2014) 1927.
[7] B. Li, D. Louca, B. Hu, J.L. Niedziela, J. Zhou, J.B. Goodenough, J. Phys. Soc. Jpn. 83 (2014) 084601.
[8] W.P. Davey, Phys. Rev. 21 (1923) 143.
[9] A.D.B. Woods, W. Cochran, B.N. Brockhouse, Phys. Rev. 119 (1960) 980.
[10] M. Kempa, P. Ondrejkovic, P. Bourges, J. Olliver, S. Rols, J. Kulda, S. Margueron, J. Hlinka, J. Phys.: Condes. Matter 25 (2013) 055403.
[11] M. Kempa, P. Ondrejkovic, P. Bourges, P. Marton, J. Hlinka, Phys. Rev. B 89 (2014) 054308.
[12] M.E. Manley, A.J. Sievers, J.W. Lynn, S.A. Kiselev, N.I. Agladze, Y. Chen, A. Llobet, A. Alatas, Phys. Rev. B 79 (2009) 134304.
[13] M.E. Manley, D.L. Abernathy, N.I. Agladze, A.J. Sievers, Sci. Rep. 1 (2011) 4.
[14] M.E. Manley, J.R. Jeffries, H. Lee, N.P. Butch, A. Zabalegui, D.L. Abernathy, Phys. Rev. B 89 (2014) 224106.
[15] A.J. Sievers, M. Sato, J.B. Page, T. Rössler, Phys. Rev. B 88 (2013) 104305.
[16] R. Kajimoto, M. Nakamura, Y. Inamura, F. Mizuno, K. Nakajima, S. Ohira-Kawamura, T. Yokoo, T. Nakatani, R. Maruyama, K. Soyama, K. Shibata, K. Suzuya, S. Sato, K. Aizawa, M. Arai, S. Wakimoto, M. Ishikado, S. Shamoto, M. Fujita, H. Hiraka, K. Ohoyama, K. Yamada, C.H. Lee, J. Phys. Soc. Jpn. 80 (2011) SB025.

[17] M. Nakamura, R. Kajimoto, Y. Inamura, F. Mizuno, M. Fujita, T. Yokoo, M. Arai, J. Phys. Soc. Jpn. 78 (2009) 093002.
[18] Y. Inamura, T. Nakatani, J. Suzuki, T. Otomo, J. Phys. Soc. Jpn. 82 (2013) SA031.